Rapid-acting antidepressants ketamine and nitrous oxide converge on MAPK-DUSP signaling in the medial prefrontal cortex

Stanislav Rozov[1,2], Roosa Saarreharju[1,2], Stanislav Khirug[3], Markus Storvik[4], Claudio Rivera[3,5] and Tomi Rantamäki[1,2*]

[1]Laboratory of Neurotherapeutics, Drug Research Program, Division of Pharmacology and Pharmacotherapy, Faculty of Pharmacy, University of Helsinki, Helsinki, Finland, 00014

[2]SleepWell Research Program, Faculty of Medicine, University of Helsinki, Helsinki, Finland, 00014

[3] Neuroscience Center, University of Helsinki, Helsinki, Finland, 00014

[4] University of Eastern Finland, Kuopio, Finland, 70029

[5] Aix Marseille Univ, INSERM, INMED, Marseille, France, 13007

* Tomi Rantamäki, Laboratory of Neurotherapeutics, Drug Research Program, Division of Pharmacology and Pharmacotherapy, Faculty of Pharmacy, University of Helsinki, Helsinki, Finland, 00014, +358-415020978

Email: tomi.rantamaki@helsinki.fi

*Stanislav Rozov, Laboratory of Neurotherapeutics, Drug Research Program, Division of Pharmacology and Pharmacotherapy, Faculty of Pharmacy, University of Helsinki, Helsinki, Finland, 00014

Email: stanislav.rozov@helsinki.fi

Abstract

Nitrous oxide (N_2O) has shown promise as a putative rapid-acting antidepressant but little is known about the underlying mechanisms. We have here performed transcriptomics and electrophysiological studies to dissect shared signatures acutely induced by 1-hour inhalation of 50% N_2O and single subanesthetic dose of ketamine, a well-established antidepressant, in the adult mouse medial prefrontal cortex. Unbiased quantitative RNA sequencing demonstrated that several transcripts belonging to the mitogen-activated protein kinase (MAPK) pathway are similarly regulated by N_2O and ketamine. In particular, both treatments increased the expression of the dual specificity phosphatases (DUSPs), negative regulators of MAPKs. N_2O also rapidly reduced saccharine preference and induced expression of *Dusp1* and *Dusp6* in animals subjected to chronic treatment with stress hormone corticosterone. Interestingly, overall, the effects of N_2O on the mRNA expression were more prominent and widespread compared to ketamine. Ketamine and to lesser extent nitrous oxide caused elevation of gamma-activity (30-100 Hz) of cortical local field potential, however firing rate and phase locking of spike-to-LFPs of neurons of this brain area showed no uniform changes across the treatments. These findings provide support for the antidepressant properties of N_2O and further highlight the involvement of MAPK regulation in the mechanism of action of rapid-acting antidepressants.

Introduction

Nitrous oxide (N_2O, “laughing gas”) has been used for several decades as an adjunct anesthetic, analgesic and anxiolytic. Recently, N_2O has shown promise as a rapid-acting antidepressant [1], presumably owing to its antagonistic effects on *N*-methyl-D-aspartate receptors (NMDARs), similar to that of ketamine. Antidepressant properties of ketamine are coupled to stimulatory effects on neural ensembles in cortical microcircuits that likely arise through the blockade of NMDARs in inhibitory interneurons and subsequent disinhibition of glutamatergic synapses and/or inhibition of pre-synaptic NMDAR on excitatory synapses of pyramidal cortical neurons, that leads to an increase in excitatory synapse drive [2], following modulation of e.g. TrkB neurotrophin and MAPK (mitogen-activated protein kinase) signaling [3]. Unlike ketamine, the knowledge about the antidepressant effects of N_2O is limited. However, our recent animal studies indicate that N_2O and ketamine trigger similar time-dependent effects on molecular signaling in the cortex. Specifically, an acute increase in MAPK signaling is subsequently followed by a brain state characterized by slow-wave EEG activity, which we have associated with increased TrkB signaling and reduced phosphorylation of MAPK [4].

Here we have performed electrophysiological and molecular analyses of prefrontal cortices of adult mice, treated with subanesthetic dose of ketamine or a clinically relevant dosing regimen of N_2O. Multiunit activity (MUA) as well as phase coupling analyses showed heterogeneity in responses to treatment in putative pyramidal- and interneurons. Within treatment gene-wise comparisons revealed that both treatments acutely converge on MAPK pathway, of which the dual specificity phosphatases (DUSPs) emerged as most clear hits. N_2O also rapidly counteracted reduced saccharine preference and induced expression of *Dusp1* and *Dusp6* in animals subjected to chronic treatment with stress hormone corticosterone, a model of depression [5]. These findings provide further support for the antidepressant properties of N_2O and highlight the involvement of MAPK regulation for NMDAR blocking antidepressants.

Materials and Methods

Animals

Eight-to-ten weeks old male C57BL/6JOlaHsd mice (Envigo, Netherlands) were used. Animals were single-housed in sound-proof cages (Scantainer, Scanbur, Sweden) under controlled conditions (22 ±1°C, 12-h light-dark cycle, 6 AM lights on) in the animal facility of the University of Helsinki with free access to food and water, unless mentioned otherwise. Treatments and behavioral tests, excluding the saccharin preference test, were performed during the light phase (*Zeitgeber Time*, ZT 3-7). The experiments were carried out according to the guidelines of the Society for Neuroscience and were approved by the County Administrative Board of Southern Finland (License: ESAVI/5844/2019).

Drug treatments

Ketamine-HCl (Ketaminol®, Intervet International B.V., 511485) was diluted in saline and injected intraperitoneally (i.p.) at a dose 10 mg/kg [6] (injection volume ~10 ml/kg). Controls received saline. A 1:1 mixture of N_2O and O_2 (Livopan®, Linde Healthcare, Finland), was administered for 40-60 minutes similarly to previous clinical [1] and animal [4] studies. Since RNAseq experiment included one control group for both ketamine and N_2O treatments, saline (i.p.) was given to both control and N_2O group to control for the effects of injection. To control for potential effect of hyperoxygenation in 50% N_2O, additional study utilized 50% N_2/50% O_2 mixture.

Collection of brain samples

For the biochemical analyses the animals were euthanized by cervical dislocation at two hours after ketamine/saline injections or two hours after the onset of 1-hour N_2O treatment. Bilateral medial prefrontal cortex (mPFC; including prelimbic and infralimbic cortices) was rapidly dissected on a cooled dish [7] and stored at -80 °C until further processing.

RNA sequencing

Extraction of mRNA was done with NucleoSpin RNA plus (Macherey-Nagel, Germany) kit in accordance with manufacturer's instructions. RNA integrity was tested prior to sequencing with Bioanalyser (Agilent Technologies, USA) and samples with RIN>9.0 were used in analysis. Samples were sequenced with Illumina NextSeq sequencer (Illumina, San Diego, CA, USA) at the Biomedicum Functional Genomics Unit (FuGU) in High output runs using NEBNext® Ultra™ II Directional RNA Library Prep Kit for Illumina 3. The sequencing was performed as single-end sequencing for read length 75 bp (SE75 or 1x75bp).

Data processing steps included FastQC quality analysis, analysis summarization with MultiQC [8], light quality trimming with Trimmomatic [9], alignment of the sample reads against the mouse GRCm38.p6 (GCA_000001635.8) reference with STAR [10], spliced transcripts alignment to a reference genome, mapping quality assessment with Qualimap [11], read quantification (featureCounts, [12]), differential expression statistics (negative binomial linear model followed by Wald's test, followed by Benjamini-Hochberg correction for multiple comparisons implemented in DESeq2 R-library [13]. To identify molecular processes primarily affected by ketamine or N_2O alone gene expression data (Wald's test, $p_{adj}<0.05$) were subjected to gene ontology search (GO, [14]) and pathways that exceeded significance threshold (Fisher's exact test, $p_{adj}<0.05$) were considered as significantly enriched. To find common molecular signatures of ketamine and N_2O effects, signed $\log_{10}(P)$ values from the previous step were used in rank-rank hypergeometric overlap (RRHO) analysis as described earlier (step size=100) [15]. *A-posteriori* power analysis with alpha=0.1 and beta=0.25 [16] was used as selection criterion for commonly regulated subset of genes identified by RRHO (signed $\log_{10}(P)$ values higher than maximum estimated co-occurrence rate), to be included in GO search as described above. Genes, that belonged to several pathways and had >1.5 times difference vs. control (Wald's test, $p_{adj}<0.05$) were selected for qPCR validation analysis.

Quantitative RT-PCR

mRNA extraction was done with NucleoSpin RNA plus (Macherey-Nagel, Germany) kit according to manufacturer's instructions. The concentration and purity of RNA was assessed with the Nanodrop 2000 Spectrophotometer (Millipore, USA). Samples with RNA concentration > 100 ng/µl, 260/280 nm ratio > 1.9 and 260/230 nm ratio > 1.9 were processed for cDNA synthesis (one sample excluded) with the Maxima First Strand cDNA Synthesis Kit and dsDNase mix (K1672, Thermo Scientific, USA). The primers used to amplify specific cDNA regions of the transcripts are listed in **Supplementary Table 1**. Primers for *Dusp1*, *Dusp5*, *Dusp6,* and *Nr4a1* were designed using PrimerBLAST service (NCBI, USA) and tested for specificity and selectivity. Amplification of cDNA and corresponding control samples was done with Maxima SYBR Green/ROX qPCR Master Mix (2X) (K0221, Thermo Scientific, USA) on the Lightcycler® 480 System (Roche, Switzerland). Relative quantification of templates was performed as described in

[17], with cDNA data being normalized to the joint *Gapdh* and *beta-actin* transcripts' levels. Amplification efficiencies of PCR reactions were estimated by dilution series: *Gapdh*: 1.93; *Actb*:1.88, *Fos*: 1.84, *Nr4a1*: 1.91, *Arc*: 1.98, *Dusp1*:1.99, *Dusp5*: 2.04, *Dusp6*: 1.97.

Electrophysiological recording and data analysis

Craniotomy for electrophysiological recording along with montage of metal frame for head fixation was performed under isoflurane anesthesia (5% induction, 2% maintenance), accompanied by analgesic (carprofen, s.c. 5 mg/kg) and local analgesia (lidocaine). To facilitate administration of injectable compounds during recording session such subjects were additionally implanted with catheter connected to injection port (s.c.). Animals were recovered for 7 days followed by 4 days of habituation to Mobile HomeCage (Neurotar, Helsinki, Finland). Recordings were performed in the anterior cingulate cortex (AP: -2.0, ML: 0.75, angle 45°) on head-restrained conscious subjects with A4x8-5mm-100-200-177-A32 probe (Neuronexus, USA) connected to A32 preamplifier and SmartBox Pro amplifier (Neuronexus, USA). A face mask was used for the delivery of gaseous substances. Data acquisition was performed at a sampling rate 20 kHz-30 kHz. Forty minutes after control treatment subjects received either ketamine or N_2O and recording continued for 40 min. Probe locations were verified after the experiment on brain slices under fluorescent microscope.

Spike sorting was performed on band-pass filtered (300-5000 Hz, Butterworth filter, order 3), whitened, median-subtracted data by SpykingCircus software [18]. Results of spike sorting were manually verified using Phy2 software to identify putative pyramidal- and interneuron-like spikes based on duration of after-hyperpolarization phase and inter-spike intervals. Spike-to-local field potential (LFP) coupling, firing rate assessment and statistical analyses (omnibus test to assess spike-to-LFP phase lock of single neurons (single unit activity, SUA) or their small groups (multiunit activity, MUA), Watson-Williams test to assess significance of treatment-induced spike-to-LFP phase lock change of multiple S/MUA, paired T-test to assess significance of treatment-induced firing rate change) were performed in Matlab (Nattick, USA) with CircStat toolbox [19].

Chronic corticosterone administration

Corticosterone (CORT; catalog no. 46148, Sigma, USA) was dissolved in 99,5% ethanol, and further in tap water to yield concentration of 100 µg/ml of CORT (ethanol 1%). Mice were habituated for a week before starting the administration. Mice were exposed to either CORT solution or 1% ethanol as control in place of drinking water for 26 days. Solutions were presented to mice in two 15 ml tubes, with tips cut to a size which allowed drinking but minimized leakage. The weight of the drinking tubes was recorded daily at ZT5-7 to monitor drinking. The solutions were replaced every three days.

Coat assessment

The scoring of coat state was carried out by the assessment of eight different body parts: head, neck, dorsal coat, ventral coat, tail, fore paws, hind paws and genital region. A score of either 0 for a coat in a good state or a score of 1 for a dirty and unkempt coat were given for each of these areas. The total score for an individual mouse was obtained from the sum of the score of each of its body parts [20].

Saccharin preference test (*SPT*)

SPT examines the animal's capacity to experience hedonic pleasure evoked by sweet solutions. Mice had been habituated to the presence of drinking tubes. On the test day, drinking was restricted for eight hours (ZT 5:30-12:30) prior to testing. Saccharin solution was prepared immediately before testing, by dissolving saccharin sodium salt hydrate (S1002-500G, Sigma, USA) in tap water to make 0.1% (w/v) solution. The mice were then given saccharin solution in one tube and water in the other tube for four hours (ZT 12:30-16:30). Water consumption and saccharin solution consumption were calculated by weighing the tubes before and after the four-hour testing period. Saccharin preference was determined by calculating the fraction (%) of saccharin water consumption divided by total water consumption.

Tail suspension test (*TST*)

For the TST each mouse was brought into the test room for 30 min of acclimatization before the start of its test. Mice were recorded with Ethovision XT (Noldus, Netherlands) for 6 min while suspended from their tail 15 cm from the top of a compartment measuring 30 cm in height using lab tape. A small plastic tube was placed around the base of the tail to prevent tail climbing. The behavioral apparatus was cleaned with water between animals. Normalization, assessment of total immobility time and latency was done in Matlab (MathWorks, Nattick, USA).

Statistics

Statistics were calculated using the R software (version 3.5.2, [21]). Differences among experimental groups in qPCR analysis were determined by either two-tailed non-paired T-test or one-way analysis of variance (ANOVA), followed by Tukey *post-hoc* test with Bonferroni correction. Differences among experimental groups in behavioral tests were determined by either Kruskal–Wallis test or one-way multivariate ANOVA (MANOVA). Differences in coat assessment were determined by Kruskal–Wallis test followed by Dunn's Multiple Comparison *post-hoc* test with Bonferroni correction if significant. A one-way MANOVA conducted for SPT and TST data was followed by univariate one-way ANOVAs and subsequent Tukey *post-hoc* test with Bonferroni correction. P values <0.05 were considered statistically significant.

Results

Electrophysiological effects of treatments with ketamine and N_2O

To characterize acute functional responses to subanesthetic-dose ketamine and 50% N_2O we first examined their effects on local field potentials, firing rate and spike-to- LFP coupling of S/MUA in the anterior cingulate cortex (ACC). Ketamine (**Figure 1B**) considerably elevated gamma-activity (30-100 Hz) in the ACC, whereas N_2O (**Figure 1C**) did so to much less extent. In addition, strong enhancement of 7 Hz band and suppression of 10 Hz one was induced by N_2O. Spike sorting identified two major extracellular electrophysiological responses that are characteristic to putative pyramidal- (**Figure 1D**) and interneuron (**Figure 1G**) cell types. Nearly 70% of putative pyramidal S/MUA increased their firing rate in response to ketamine treatment (**Figure 1E**; p=0.07, paired T-test), whereas only 40% did so in N_2O-treated group (**Figure 1F**; p=0.76, paired T-test). Moreover, about 80% of interneuron-like S/MUA in ketamine-treated (**Figure 1H**; p=0.22, paired T-test) and 45% of that in N_2O-treated (**Figure 1I**; p=0.25, paired T-test) group increased their firing rates. Thus, both putative pyramidal neurons and interneurons generally tend to exhibit more firing in response to ketamine and N_2O, although the responses were not completely uniform.

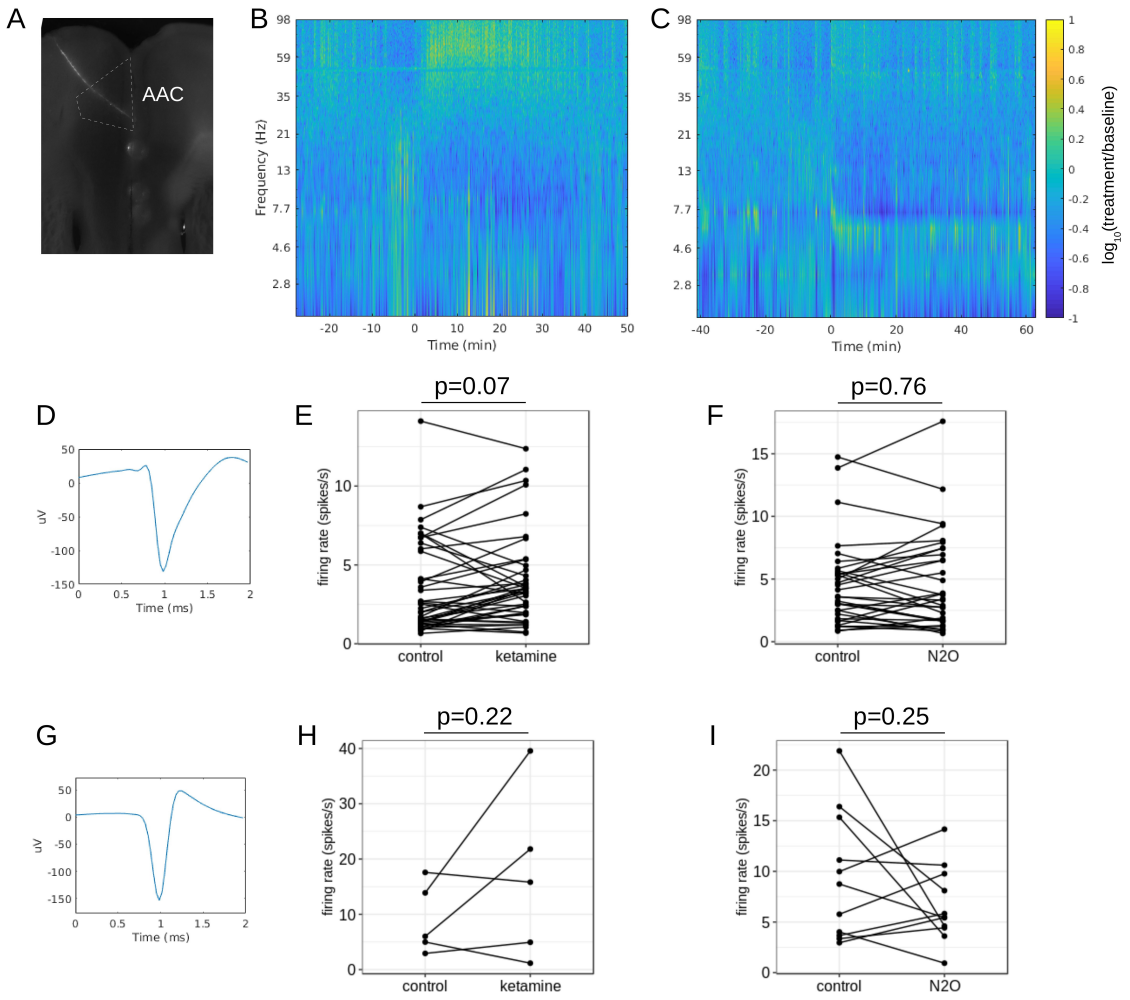

Figure 1. Effects of ketamine (10 mg/kg, i.p,) or 50% N_2O / 50% O_2 on local field potentials and firing rates of putative pyramidal- and interneurons of the anterior cingulate cortex. (A) Fluorescent tracer DiI was used to visualize probe location. Gamma-activity (30-100 Hz) considerably elevated in the ACC in response to ketamine (time 0-50 min; **B**), whereas N_2O (time 0-60 min; **C**) did so to much less extent. Putative pyramidal- (**D**) and interneurons (**G**) were identified based on their spike shapes. Majority of these units increased firing rate in response to ketamine (**E** and **H** respectively), whereas only 40-45% did so in N_2O-treated subjects (**F** and **I,** respectively). The number of subjects was n=4 (N_2O) and 3 (ketamine); total number of units was 36 (N_2O) and 40 (ketamine).

Spectral analysis of the vicinity of spikes revealed dominant 3 Hz and in some cases 7 Hz oscillations. Subsequent spike-to-LFP phase analysis followed by omnibus test (histogram of spike-to-LFP phase distribution; **Supplementary figure 1E**) showed that nearly half of putative pyramidal SUA/MUA either coupled to dominant 3 Hz rhythm irrespective of treatment with

ketamine (**Supplementary figure 1A**; p=0.83, Watson-Williams test) or N_2O (**Supplementary figure 1B**; p=0.76, Watson-Williams test) groups or lost/developed coupling to that frequency in response to treatment. The other half of these S/MUA did not demonstrate coupling to any of LFP frequencies (**Supplementary Table 2**). In turn, virtually all interneuron-like S/MUA had strong coupling to dominant 3 Hz frequency, that was nevertheless not altered by neither ketamine (**Supplementary figure 1C**; p=0.56, Watson-Williams test) nor N_2O (**Supplementary figure 1D**; p=0.56, Watson-Williams test).

To examine changes in transcriptome induced by ketamine or N_2O (60 min administration) we conducted transcriptome-wide analysis of samples derived from mPFC 2 hours after treatment onset (**Figure 2A**). **Figure 2B-C** shows 25 most significantly upregulated and 25 most significantly downregulated genes between saline and ketamine and saline and N_2O groups. Gene-wise comparisons of saline vs. ketamine groups (16968 transcripts) revealed 15 differentially expressed genes (Wald's test, $p_{adj}<0.05$): *Dusp5*, *Dusp6*, *Erf, Etv6, Fam84b, Ier5l, Junb, Kdm6b, Klf10, Lrtm2*, *Nr4a1*, *Sox8*, *Spry4, Tiparp,* and *Wisp1*. In contrast, out of 15257 genes analyzed in N_2O vs saline groups, about 740 genes reached significance level of regulation. GO analysis showed only 2 biological processes regulated by ketamine and 18 processes affected by N_2O (**Table 1**). Notably, MAPK cascade, was regulated by both treatments.

Substantial part of the pathways and gene transcripts influenced by N_2O are implicated in synaptic function and neuronal activity (**Table 1**). This treatment regulated synaptic vesicle trafficking factors (*Apba1*, *Cplx1*, *Stxbp2*, *Syt13*, *Snap25*, *Unc13a*, *Picalm*, *Dnm3*), G-protein-coupled receptors (*Adgrl1*, *Chrm4*, *Gpr3*, *Htr1a*, *Htr2a*, *Htr6*, *Lpar1*, *Mc4r* and *Ptger4*) and GABA-A receptor subunits (*Gabra2* and *Gabra3*). We also observed downregulation of expression of postsynaptic scaffold factors such as *Nlgn2*, *Nlgn3*, *Shank3*. Moreover, several immediate-early genes were regulated, including *Arc*, *Egr1*, *Egr2*, *Egr4*, *Fos*, *Fosb*, *Junb*, *Klf4*, *Maff* and *Nr4a1*. Notably, 4 out of 10 known dual-specificity serine-threonine phosphatases (*Dusp*) which are principal negative regulators of three main pathways of MAPK signaling cascade - JNK (*Dusp1, Dusp4*), p38-MAPK (*Dusp1*) and MAPK (*Dusp5*, *Dusp6, Dusp4*) - were regulated by N_2O.

We further analyzed concordance/discordance in mRNA changes in the mPFC induced by ketamine and N_2O by using RRHO analysis. Non-corrected results of Wald's tests from the previous step were submitted to RRHO analysis which revealed ~1600 genes, with highest estimated probability of co-occurrence between these treatments (**Figure 1D**, $p=10^{-128}$). A subset of these genes, chosen based on *a posteriori* power analysis (alpha=0.1, beta=0.25, 125 genes), were further processed to GO search. Again, several genes that were significantly influenced by both treatments are known members of MAPK as well as a subset of immediate early genes (**Table 1**).

Table 1. Results of gene ontology analysis of genes, which expression level in response to treatment with N_2O/O_2 and/or ketamine significantly changed compared to control (Wald's test, $p<0.05$).

Biological Process (PANTHER GO-Slim)	over/ under	Fold enrichment	raw P-value	FDR
N_2O/O_2 (50%/50%, 60 min)				
epidermal cell differentiation (GO:0009913)	+	16.22	< 0.001	0.007
circadian regulation of gene expression (GO:0032922)	+	12.16	< 0.001	0.001
'de novo' protein folding (GO:0006458)	+	7.21	0.004	0.045
transforming growth factor beta receptor signaling pathway (GO:0007179)	+	6.28	0.001	0.014
cellular response to peptide hormone stimulus (GO:0071375)	+	5.16	0.001	0.014
synaptic vesicle cycle (GO:0099504)	+	4.42	< 0.001	0.009
autophagosome assembly (GO:0000045)	+	4.32	0.004	0.046
response to abiotic stimulus (GO:0009628)	+	3.96	< 0.001	0.005
heart development (GO:0007507)	+	3.72	0.004	0.047
central nervous system development (GO:0007417)	+	3.37	0.004	0.045
MAPK cascade (GO:0000165)	+	3.09	< 0.001	0.008
transmembrane receptor protein serine/threonine kinase signaling pathway (GO:0007178)	+	3.07	0.004	0.046
neuron projection morphogenesis (GO:0048812)	+	2.57	0.002	0.027
G protein-coupled receptor signaling pathway, coupled to cyclic nucleotide second messenger (GO:0007187)	+	2.48	0.004	0.042
chemical synaptic transmission (GO:0007268)	+	2.36	0.001	0.017
positive regulation of cellular protein metabolic process (GO:0032270)	+	2.01	0.004	0.047
regulation of transcription, DNA-templated (GO:0006355)	+	1.72	< 0.001	< 0.001
immune response (GO:0006955)	-	0.44	0.003	0.039
Ketamine (10 mg/kg, i.p.)				
tissue morphogenesis (GO:0048729)	+	84,9	< 0.001	0.0193
MAPK cascade (GO:0000165)	+	32,05	< 0.001	0.0123
N_2O/O_2 and ketamine (RRHO analysis)				
MAPK cascade (GO:0000165)	+	10.5	< 0.001	< 0.001
regulation of transcription, DNA-templated (GO:0006355)	+	2.48	< 0.001	< 0.001
apoptotic process (GO: 0006915)	+	6,72	< 0.001	0.018
regulation of cell cycle (GO: 0051726)	+	5.54	< 0.001	0.0027

To validate the RNAseq findings, we chose selected transcripts for qPCR analysis. The expression levels of *Dusp1, Dusp5, Dusp6* and *Nr4a1* were significantly increased by both ketamine and N2O while only N2O increased expression of *Fos* and *Arc* (**Figure S2A**). Notably, in these experiments we compared N2O to non-treated (air) control group which rises question on effect of 50% O2 on target genes. To address this concern, we compared expression of *Dusp1*, *Dusp*5 and *Dusp*6 between 50% N2O / 50% O2 and 50% N2 / 50% O2 groups and found no differences between them (**Figure S2B**).

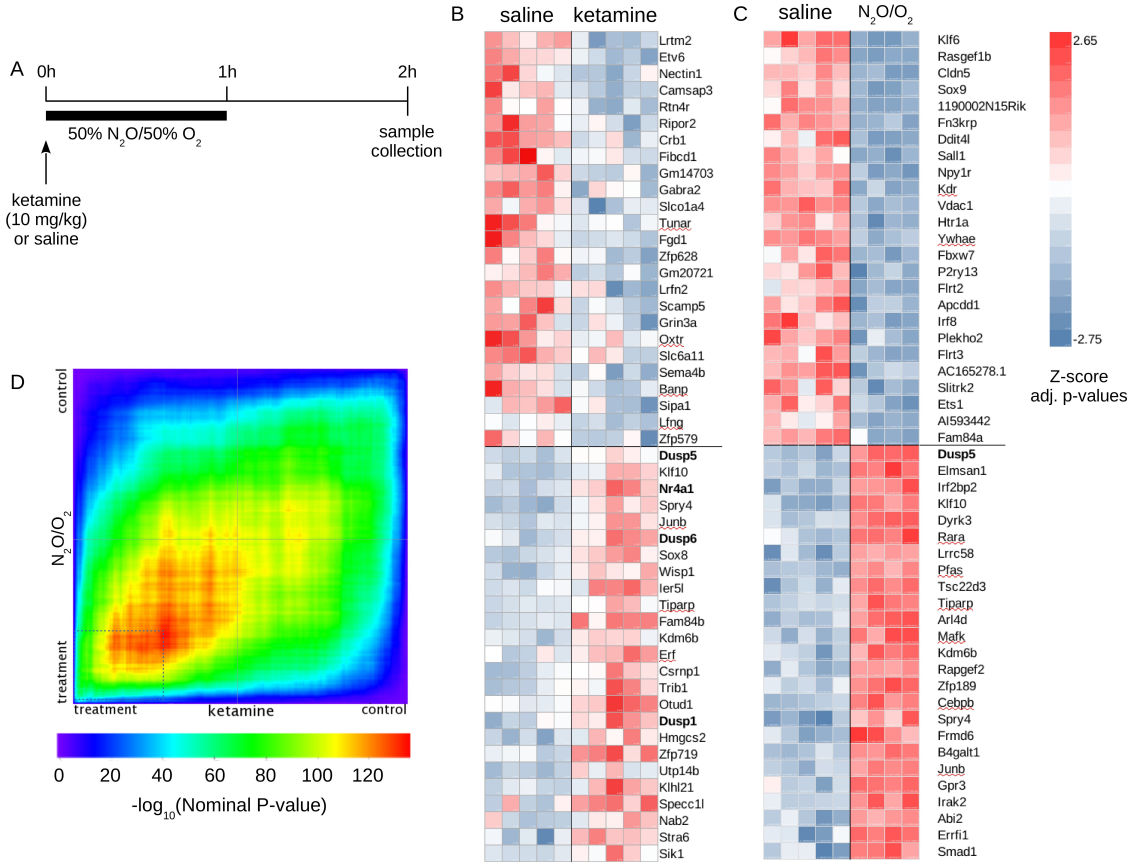

Figure 2. Results of RNAseq analysis of N2O- and ketamine-treated groups of animals in comparison to control treatment. *(**A**) Schematic overview of the experiment. Male C57BL/6J mice were administered with saline (n=5), ketamine (10 mg/kg, i.p. n=5) or 50% N2O (60 min, n=4). Two hours after beginning of administration, samples were collected from the medial prefrontal cortex for further analyses. (**B-C**) Heatmap representation of expression levels of 25 most significantly upregulated and 25 most significantly downregulated genes between saline and ketamine (**B**) and saline and N2O (**C**) groups. Normalized count values are represented as Z-scores. (**D**) Rank-rank hypergeometric overlap (RRHO) map representing shared mRNA*

changes in the adult mouse medial prefrontal cortex in response to control vs. ketamine and control vs. N_2O treatments. Thin dashed line represents highest estimated probability of co-occurrence between these treatments ($p=-log_{10}128$).

N_2O elicits antidepressant-like effects and up-regulates Dusps in mice subjected to chronic CORT

We next examined whether N_2O, and ketamine, bring along antidepressant effects and regulate *Dusp* expression in animals exhibiting depression-like state. For this we selected corticosterone stress model (5), which has been previously exploited to investigate the mechanisms underlying ketamine´s antidepressant actions. Indeed, chronic (26 days) CORT exposure (0.10 mg/ml in drinking water) recapitulated certain depression-related behaviors, including worsened coat state and reduced saccharin preference, although behavior (mobility) in the tail suspension test was unaffected (**Figure 3A-D**). Importantly, treatment with 50% N_2O (60 min), and a single subanesthetic-dose ketamine, increased saccharine preference, which was assessed for a total duration of 4 hours in the following active period (i.e. dark phase). The treatments did not affect coat state that was assessed approximately 24 h after the drug treatments.

Another cohort of CORT mice were subjected to acute treatments with ketamine and 50% N_2O, and mPFC samples for qPCR analyses were collected 2 h after. N_2O increased expression of *Dusp1* and *Dusp6* (**Figure 3E**). N_2O tended to increase also *Arc* and *Nr4a1* expression but the effect was significant only when compared to animals which received no CORT treatment (**Figure 3E**). Unexpectedly, ketamine treatment or CORT administration itself was not associated with significant changes in any of the transcripts in this experiment (**Figure 3E**).

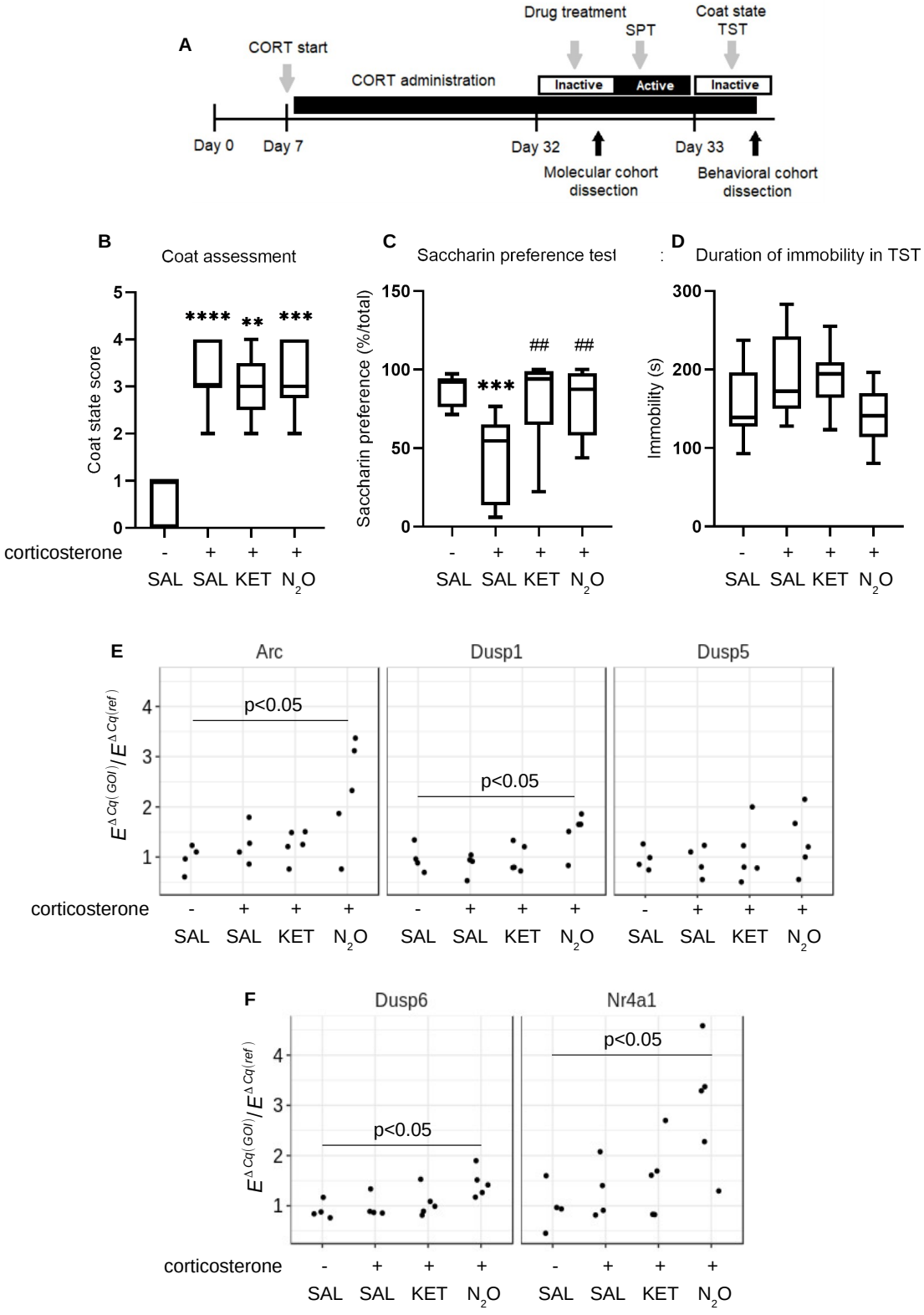

Figure 3. Effects of 50% N_2O and ketamine (10 mg/kg, i.p.) in the corticosterone-induced depression-like state and Dusp expression *A) Experimental design.* ***B****) Coat assessment 24h after drug treatments. (****C****) Saccharin preference during the first 4 hours of the dark phase on the same day as drug treatments. (****D****) Total immobility time in TST 24 h after drug treatments. Boxplots depict the median, interquartile range, and minimal and maximal values.* ***E****) Levels of Dusp1, Dusp5, Dusp6, Arc and Nr4a1 in the medial prefrontal cortex 2h after onset of drug treatments. Columns depict mean±SEM. Compared to control group (NO CORT VEH) = *<0.05, **<0.01, ***<0.005, ****<0.001. Compared to CORT VEH = #<0.05, ##<0.01.*

Discussion

N_2O has shown promise as a putative rapid-acting antidepressant [1] and has several favorable translational properties compared to ketamine: N_2O can only be administered by inhalation, does not undergo biotransformation [22] and shows relatively similar pharmacokinetics between mammalian species. However underlying mechanisms remain poorly studied. Our comparative RNA screening analysis of mouse medial prefrontal cortex - a brain area recognized for its role in the development of depressive states in humans and animal models of depression [23] - suggests that effects of 50% N_2O and subanesthetic-dose of ketamine converge on MAPK signaling pathway. In particular, both treatments upregulated the expression of *Dusp*s, negative regulators of MAPK signaling. This cascade has been consistently linked with antidepressant effects of ketamine [24], and both MAPK and DUSPs are also activated by non-pharmacological treatments of depression such as electroconvulsive shock (a model of electroconvulsive therapy) [25]. Previous transcriptomic studies on ketamine-treated subjects have been previously performed [26–28] but, although multiple factors including different brain structures used and differences in experimental design (e.g. inclusion of behavioral tests) complicate their direct comparison with the current work, MAPK pathway have been highlighted by one of the reports [28].

Recently we demonstrated N_2O-mediated elevation of *Dusp1* (*MKP1; [4]*), however, no consensus is reached concerning the effects of ketamine on this target, as it has been shown to be either upregulated [26] or downregulated [28] in the prefrontal cortex of rodents. On the contrary, MAPK pathway (ERK1/2) inhibitors have been shown to cause depressive-like behavior [29] and the phosphorylation of MAPKs is altered in depressed patients and in animal models of depression [30]. Moreover, inhibition of ERK1/2 activity blocks antidepressant-like behavioral effects of antidepressant drugs including ketamine [31].

The ability of ketamine to regulate MAPK kinases is likely connected to its stimulatory effects on neural ensembles in cortical microcircuits [32]. These effects are suggested to arise through the

blockade of NMDARs in either inhibitory interneurons and subsequent disinhibition of glutamatergic synapses or direct inhibition of pre-synaptic NMDARs on excitatory synapses of pyramidal cortical neurons, that leads to an increase in excitatory synapse drive [2]. Activation of *Dusps* by N_2O may be related to either its ability to block NMDARs [33] or its interaction with serotonergic [34], noradrenergic [35] receptors and cation channels [36].

Diversity of targets of N_2O suggests complex response mechanism of CNS to this compound. Indeed, along with several transcripts belonging to the MAPK pathway, treatment with N_2O affected hundreds of other transcripts including synaptic vesicle trafficking factors (*Apba1*, *Cplx1*, *Stxbp2*, *Syt13*, *Snap25*, *Unc13a*, *Picalm*, *Dnm3*), G-protein-coupled receptors (*Adgrl1*, *Chrm4*, *Gpr3*, *Htr1a*, *Htr2a*, *Htr6*, *Lpar1*, *Mc4r* and *Ptger4*), ion channels (*Gabra2* and *Gabra3*), postsynaptic scaffold factors (*Nlgn2*, *Nlgn3*, *Shank3),* and immediate early genes (*Arc*, *Egr1*, *Egr2*, *Fos Egr4*, *Fosb*, *Junb*, *Klf4*, *Maff* and *Nr4a1),* which may be controlled by neuronal activity and subsequent activation of MAPK (35). In contrast, effects of ketamine were much less prominent. However, one of the hits, *Nr4a1* (also known as *Nurr77*), has also previously been shown to be upregulated by ketamine in primary neuronal cultures [37].

Current study demonstrated elevation of high frequency (>30 Hz) cortical LFPs in response to ketamine and N_2O treatment which is in line with several reports on human and rodents [4,38]. In addition, strong enhancement of 7 Hz band and suppression of 10 Hz one was induced by N_2O. To bridge these macroscopic EEG observations to S/MUA recorded, we assessed S/MUA in relation to LFP registered at the same location and time. Spike-to-LFP coupling analysis showed that although 3 Hz oscillation dominated in the vicinity of spikes of all analysed S/MUA, units that demonstrated persistent coupling to this oscillation were neither synchronous nor changed in response to treatment with either compound. Additionally, a small fraction of S/MUA had second dominant frequency at 7 Hz, which is likely related to increase of its power seen at spectrograms. Another interesting observation, that is yet to be explained is stronger coupling of putative interneurons to 3 Hz activity than that of pyramidal cells. Slow oscillations during wakefulness in anterior cortical areas has been attributed to activity of several circuits. Recent reports [39] show strong phase-locked spiking activity of orbitofrontal neurons to 4 Hz rhythm of respiration. However, similarly to our finding, Kőszeghy and colleagues [40] demonstrated modest phase locking of mPFC neurons to this rhythm with no phase preference throughout their population. Another interpretation could come from synchronization of cortico-amygdalar circuit, which is related to fear response [41], or cortico-VTA-hypothalamic circuit, which may be related to working memory [42].

We further observed firing rate elevation of majority of recorded putative pyramidal cells in response to ketamine, which matches to observed elevation of gamma activity, agrees with recent studies [43], and align with the inhibition-disinhibition hypothesis [2]. However, in addition

to these cells, spiking frequency of a fraction of interneuron-like S/MUA also increased whereas the firing rate of the rest of them declined modestly. In contrast no increase in firing rate of putative pyramidal cells was observed in N_2O-treated group. Because of the small number of recorded responses from putative interneurons, that reflects overall low relative quantity of these cells in cerebral cortex, it is not possible to generalize observed effects to their whole population. Nevertheless, our data show heterogeneity in responses of both cell types in response to ketamine and clear differences between both treatments in firing rate response suggesting more complex relationships within and between local circuits than simple on-off response. Recording with higher electrode density and quantity accompanied by optogenetic stimulation/inhibition of selected cell types would not only provide certainty in cell types under investigation, including types of interneurons, but be essential to reveal changes in connectivity of local cortical circuits in response to treatments.

Antidepressant-like behavioral effects of N_2O have been sparsely studied in animals. Recently Liu and colleagues [44] demonstrated promising effects with repeated dosing regimen of N_2O in naïve mice. In turn our study examined the effects of N_2O in an animal model of depression. N_2O and ketamine significantly rescued reduced saccharin preference caused by chronic corticosterone exposure. N_2O, but not ketamine, also upregulated *Dusp1* and *Dusp6* mRNA expression in the mPFC in animals exposed to corticosterone. Notably, we have previously shown N_2O to elicit time-dependent phosphorylation on ERK1/2 (also known as p42/p44-MAPK) [4]. Interestingly, unlike N_2O, none of the analyzed mRNA targets of ketamine, showed significant changes between the control phenotype and corticosterone groups. Although the source of this phenomenon is unknown we speculate that interaction between treatments might have taken place. Previous studies have shown that *Dusps* and *Nr4a1* were upregulated in animal models of depression, although the results vary depending on brain region and method used to create the model [29,45,46]. Expression of *Arc* was downregulated in the frontal cortex and CA1 area of the hippocampus after both chronic mild stress and in a genetic animal model of depression [47].

Collectively these findings provide important insights into the antidepressant properties of N_2O and especially highlight MAPK signaling as a shared target for NMDAR blocking rapid-acting antidepressants.

Funding and disclosure

The authors report no competing interests.

Acknowledgments

We are grateful to personnel at the animal facility of the University of Helsinki for helping to conduct animal experiments and take care of the animals. We would like to thank the Mouse

Behavioral Phenotyping Facility (MBPF) at the University of Helsinki for providing equipment and professional assistance for behavioral testing and mouse model implementation and Functional Genomics Unit (FUGU), University of Helsinki for assistance with RNAseq data analysis. Additionally, Okko Alitalo and Dr. Samuel Kohtala are thanked for helping to conduct the experiments and to improve the manuscript. S.R. received funding from the Academy of Finland. T.R. received funding from the Academy of Finland, Business Finland and Sigrid Jusélius Foundation. S.K. and C.R. received funding from the Academy of Finland, Eranet Neuron III program and ANR project. The funding sources were not involved in writing or decision to submit the work.

Author Contributions

S.R., R.S. and T.R. planned the experiments; S.R., R.S. carried out research; S.R., R.S. prepared the figures; S.R., R.S. run statistical tests; S.K. and C.R. assisted with electrophysiological experiments and corresponding data analysis, M.S. assisted with the pathway analyses and interpretation of the RNA sequencing data; S.R. and T.R. wrote the manuscript; S.R., C.R. and T.R. provided funding; all authors commented the manuscript and accepted final submitted version.

References

1. Nagele P, Duma A, Kopec M, Gebara MA, Parsoei A, Walker M, et al. Nitrous Oxide for Treatment-Resistant Major Depression: A Proof-of-Concept Trial. Biol Psychiatry. 2015;78:10–18.
2. Miller OH, Moran JT, Hall BJ. Two cellular hypotheses explaining the initiation of ketamine's antidepressant actions: Direct inhibition and disinhibition. Neuropharmacology. 2016;100:17–26.
3. Kohtala S, Alitalo O, Rosenholm M, Rozov S, Rantamäki T. Time is of the essence: Coupling sleep-wake and circadian neurobiology to the antidepressant effects of ketamine. Pharmacol Ther. 2021;221:107741.
4. Kohtala S, Theilmann W, Rosenholm M, Penna L, Karabulut G, Uusitalo S, et al. Cortical Excitability and Activation of TrkB Signaling During Rebound Slow Oscillations Are Critical for Rapid Antidepressant Responses. Mol Neurobiol. 2019;56:4163–4174.
5. Gourley SL, Kiraly DD, Howell JL, Olausson P, Taylor JR. Acute hippocampal brain-derived neurotrophic factor restores motivational and forced swim performance after corticosterone. Biol Psychiatry. 2008;64:884–890.
6. Moda-Sava RN, Murdock MH, Parekh PK, Fetcho RN, Huang BS, Huynh TN, et al. Sustained rescue of prefrontal circuit dysfunction by antidepressant-induced spine formation. Science. 2019;364:eaat8078.
7. Kohtala S, Theilmann W, Suomi T, Wigren H-K, Porkka-Heiskanen T, Elo LL, et al. Brief Isoflurane Anesthesia Produces Prominent Phosphoproteomic Changes in the Adult Mouse Hippocampus. ACS Chem Neurosci. 2016;7:749–756.
8. Ewels P, Magnusson M, Lundin S, Käller M. MultiQC: summarize analysis results for multiple tools and samples in a single report. Bioinformatics. 2016;32:3047–3048.
9. Bolger AM, Lohse M, Usadel B. Trimmomatic: a flexible trimmer for Illumina sequence data. Bioinformatics. 2014;30:2114–2120.
10. Dobin A, Davis CA, Schlesinger F, Drenkow J, Zaleski C, Jha S, et al. STAR: ultrafast universal RNA-seq aligner. Bioinformatics. 2013;29:15–21.
11. García-Alcalde F, Okonechnikov K, Carbonell J, Cruz LM, Götz S, Tarazona S, et al. Qualimap: evaluating next-generation sequencing alignment data. Bioinformatics. 2012;28:2678–2679.
12. Liao Y, Smyth GK, Shi W. featureCounts: an efficient general purpose program for assigning sequence reads to genomic features. Bioinformatics. 2014;30:923–930.

13. Love MI, Huber W, Anders S. Moderated estimation of fold change and dispersion for RNA-seq data with DESeq2. Genome Biol. 2014;15:550.
14. Mi H, Muruganujan A, Ebert D, Huang X, Thomas PD. PANTHER version 14: more genomes, a new PANTHER GO-slim and improvements in enrichment analysis tools. Nucleic Acids Res. 2019;47:D419–D426.
15. Plaisier SB, Taschereau R, Wong JA, Graeber TG. Rank-rank hypergeometric overlap: identification of statistically significant overlap between gene-expression signatures. Nucleic Acids Res. 2010;38:e169.
16. Hart SN, Therneau TM, Zhang Y, Poland GA, Kocher J-P. Calculating sample size estimates for RNA sequencing data. J Comput Biol. 2013;20:970–978.
17. Pfaffl MW. A new mathematical model for relative quantification in real-time RT–PCR. Nucleic Acids Res. 2001;29:e45.
18. Yger P, Spampinato GL, Esposito E, Lefebvre B, Deny S, Gardella C, et al. A spike sorting toolbox for up to thousands of electrodes validated with ground truth recordings in vitro and in vivo. Elife. 2018;7:e34518.
19. Berens P. CircStat: A MATLAB Toolbox for Circular Statistics. Journal of Statistical Software. 2009;31:1–21.
20. Surget A, Saxe M, Leman S, Ibarguen-Vargas Y, Chalon S, Griebel G, et al. Drug-dependent requirement of hippocampal neurogenesis in a model of depression and of antidepressant reversal. Biol Psychiatry. 2008;64:293–301.
21. R core team. R: A language and environment for statistical computing. R Foundation for Statistical Computing. 2018. 2018.
22. Banks A, Hardman JG. Nitrous oxide. Continuing Education in Anaesthesia Critical Care & Pain. 2005;5:145–148.
23. Wellman CL, Bollinger JL, Moench KM. Effects of stress on the structure and function of the medial prefrontal cortex: Insights from animal models. Int Rev Neurobiol. 2020;150:129–153.
24. Humo M, Ayazgök B, Becker LJ, Waltisperger E, Rantamäki T, Yalcin I. Ketamine induces rapid and sustained antidepressant-like effects in chronic pain induced depression: Role of MAPK signaling pathway. Prog Neuropsychopharmacol Biol Psychiatry. 2020;100:109898.
25. Kodama M, Russell DS, Duman RS. Electroconvulsive seizures increase the expression of MAP kinase phosphatases in limbic regions of rat brain. Neuropsychopharmacology. 2005;30:360–371.

26. Bagot RC, Cates HM, Purushothaman I, Vialou V, Heller EA, Yieh L, et al. Ketamine and Imipramine Reverse Transcriptional Signatures of Susceptibility and Induce Resilience-Specific Gene Expression Profiles. Biol Psychiatry. 2017;81:285–295.
27. Orozco-Solis R, Montellier E, Aguilar-Arnal L, Sato S, Vawter MP, Bunney BG, et al. A Circadian Genomic Signature Common to Ketamine and Sleep Deprivation in the Anterior Cingulate Cortex. Biol Psychiatry. 2017;82:351–360.
28. Ficek J, Zygmunt M, Piechota M, Hoinkis D, Rodriguez Parkitna J, Przewlocki R, et al. Molecular profile of dissociative drug ketamine in relation to its rapid antidepressant action. BMC Genomics. 2016;17:362.
29. Duric V, Banasr M, Licznerski P, Schmidt HD, Stockmeier CA, Simen AA, et al. A negative regulator of MAP kinase causes depressive behavior. Nat Med. 2010;16:1328–1332.
30. Meller E, Shen C, Nikolao TA, Jensen C, Tsimberg Y, Chen J, et al. Region-specific effects of acute and repeated restraint stress on the phosphorylation of mitogen-activated protein kinases. Brain Res. 2003;979:57–64.
31. Duman CH, Schlesinger L, Kodama M, Russell DS, Duman RS. A role for MAP kinase signaling in behavioral models of depression and antidepressant treatment. Biol Psychiatry. 2007;61:661–670.
32. Rantamäki T, Kohtala S. Encoding, Consolidation, and Renormalization in Depression: Synaptic Homeostasis, Plasticity, and Sleep Integrate Rapid Antidepressant Effects. Pharmacol Rev. 2020;72:439–465.
33. Jevtović-Todorović V, Todorović SM, Mennerick S, Powell S, Dikranian K, Benshoff N, et al. Nitrous oxide (laughing gas) is an NMDA antagonist, neuroprotectant and neurotoxin. Nat Med. 1998;4:460–463.
34. Mukaida K, Shichino T, Fukuda K. Nitrous oxide increases serotonin release in the rat spinal cord. J Anesth. 2007;21:433–435.
35. Tyssowski KM, DeStefino NR, Cho J-H, Dunn CJ, Poston RG, Carty CE, et al. Different Neuronal Activity Patterns Induce Different Gene Expression Programs. Neuron. 2018;98:530-546.e11.
36. Gruss M, Bushell TJ, Bright DP, Lieb WR, Mathie A, Franks NP. Two-pore-domain K+ channels are a novel target for the anesthetic gases xenon, nitrous oxide, and cyclopropane. Mol Pharmacol. 2004;65:443–452.

37. Choi M, Lee SH, Wang SE, Ko SY, Song M, Choi J-S, et al. Ketamine produces antidepressant-like effects through phosphorylation-dependent nuclear export of histone deacetylase 5 (HDAC5) in rats. Proc Natl Acad Sci U S A. 2015;112:15755–15760.
38. Foster BL, Liley DTJ. Nitrous Oxide Paradoxically Modulates Slow Electroencephalogram Oscillations: Implications for Anesthesia Monitoring. Anesthesia & Analgesia. 2011;113:758–765.
39. Biskamp J, Bartos M, Sauer J-F. Organization of prefrontal network activity by respiration-related oscillations. Sci Rep. 2017;7:45508.
40. Kőszeghy Á, Lasztóczi B, Forro T, Klausberger T. Spike-Timing of Orbitofrontal Neurons Is Synchronized With Breathing. Front Cell Neurosci. 2018;12:105.
41. Karalis N, Dejean C, Chaudun F, Khoder S, Rozeske RR, Wurtz H, et al. 4 Hz oscillations synchronize prefrontal-amygdala circuits during fear behaviour. Nat Neurosci. 2016;19:605–612.
42. Fujisawa S, Buzsáki G. A 4 Hz oscillation adaptively synchronizes prefrontal, VTA, and hippocampal activities. Neuron. 2011;72:153–165.
43. Ali F, Gerhard DM, Sweasy K, Pothula S, Pittenger C, Duman RS, et al. Ketamine disinhibits dendrites and enhances calcium signals in prefrontal dendritic spines. Nat Commun. 2020;11:72.
44. Liu W, Li Q, Ye B, Cao H, Shen F, Xu Z, et al. Repeated Nitrous Oxide Exposure Exerts Antidepressant-Like Effects Through Neuronal Nitric Oxide Synthase Activation in the Medial Prefrontal Cortex. Front Psychiatry. 2020;11:837.
45. Gourley SL, Wu FJ, Taylor JR. Corticosterone regulates pERK1/2 map kinase in a chronic depression model. Ann N Y Acad Sci. 2008;1148:509–514.
46. Jeanneteau F, Barrère C, Vos M, De Vries CJM, Rouillard C, Levesque D, et al. The Stress-Induced Transcription Factor NR4A1 Adjusts Mitochondrial Function and Synapse Number in Prefrontal Cortex. J Neurosci. 2018;38:1335–1350.
47. Elizalde N, Pastor PM, Garcia-García AL, Serres F, Venzala E, Huarte J, et al. Regulation of markers of synaptic function in mouse models of depression: chronic mild stress and decreased expression of VGLUT1. J Neurochem. 2010;114:1302–1314.